Monolayer-Protected Clusters: Molecular Precursors to Metal Films

W. Peter Wuelfing, Francis P. Zamborini, Allen C. Templeton, Xingu Wen, Heidi Yoon,[†] and Royce W. Murray*

Kenan Laboratories of Chemistry, University of North Carolina, Chapel Hill, North Carolina 25799-3290

Monolayer-protected clusters (MPCs) are used to prepare solid, continuous metal films containing a single white metal or an alloy thereof. MPCs consist of nanoscopic metal cores coated with monolayers of thiolate ligands. In one method, multilayer films of carboxylate-functionalized alkanethiolate MPCs are assembled using Cu^{2+} coordinative bridges. The MPC film can be thermally decomposed at moderate temperature (<350 °C) to produce films of the core metal; the thiolate ligands escape as volatile disulfides. In another method, solutions of MPCs with alkanethiolate monolayers are cast or painted onto substrates, followed again by thermolysis to produce films of core metals. Films prepared from MPCs having metal alloy cores tend to exhibit metal segregation. A third method uses electrochemical generation of iodide at a Pt electrode to destabilize the MPC monolayer, an action that effectively coats the electrode with Au. The metal films are analyzed by stylus profilometry, atomic force microscopy, energy-dispersive X-ray analysis, X-ray photoelectron spectroscopy, scanning electron microscopy, and electrochemistry.

Introduction

The science and technology of thin metal film deposition is highly diverse and includes many well-established procedures. Some procedures are quite simple such as formulations for decorative metal films; most are based on methods such as chemical vapor deposition (CVD) and metal evaporation or sputtering[1,2] that are more complex and require vacuum systems and higher temperature treatments. Thin films of white metals (Au, Ag, and Pd, for example) have uses in diverse applications ranging from magnetic storage media,[3] influence on electrochemical properties,[4] conductivity,[5] and high-temperature wear-resistant/anticorrosive coatings.[6] Desirable characteristics of thin film deposition methods for these metals include use of moderate temperatures,

applicability to substrates whose surfaces have complex shapes, strong adhesion to the substrate, and simplicity. In this paper, we present new chemistry—involving nanoparticles—for white and alloy metal thin film-making that has these characteristics.

The nanoparticles employed are monolayer-protected clusters (MPCs), which are metal clusters containing from 70 to 6000 atoms coated with a dense monolayer of thiolate ligands.[7] The synthetic chemistry and properties of MPC nanoparticles have been intensely researched over the past few years by several groups,[8] including ours.[9] The stability of MPCs even in the dry state justifies the label of molecular metal film precursors used in this paper. There has been only one previous report[10] on using MPCs as precursors to metal

* To whom correspondence should be addressed.
† The University of Chicago, 5801 South Ellis Ave., Chicago, IL 60637.

(1) (a) Rossnagel, S. M. *J. Vac. Sci. Technol. B* **1998**, *16*, 2585. (b) Oskam, G.; Long, J. G.; Natarajan, A.; Searson, P. C. *J. Phys. D.: Appl. Phys.* **1998**, *31*, 1927.
(2) (a) Boyd, E. P.; Ketchum, D. R.; Deng, H.; Shore, S. G. *Chem. Mater.* **1997**, *9*, 1154. (b) Alexandrescu, R. *Appl. Surf. Sci.* **1996**, 28. (c) Jervis, T. R. *J. Appl. Phys.* **1985**, *58*, 1400. (d) Geohegan, D. B.; Edgen, J. G. *Appl. Phys. Lett.* **1984**, *45*, 1145. (e) George, P. M.; Beauchamp, J. L. *Thin Solid Films* **1980**, *67*, L25.
(3) (a) Yamada, Y.; Van Drent, W. P.; Abarra, E. N.; Suzuki, T. *J. Appl. Phys.* **1998**, *83*, 6527. (b) Ishida, A.; Miyazaki, S. *J. Eng. Mater. Technol.* **1999**, *121*, 2. Geyer, U.; von Hulsen, U.; Thiyagarajan, P. *Appl. Phys. Lett.* **1997**, *72*, 1691. (b) Kahng, S.-J.; Choi, Y. J.; Park, J.-Y.; Kuk, Y. *Appl Phys Lett.* **1999**, *74*, 1087. (c) Vernon, S. M. *Appl. Phys. Lett.* **1999**, *74*, 1382.
(4) (a) Iwamoto, N.; Chujo, H.; Akao, N.; Sugimoto, K. *J. Jpn. Inst. Met.* **1998**, *62*, 877. (b) Xhong, S.; Wang, J.; Liu, H. K.; Dou, S. X.; Skyllas-Kazacos, M. *J. Appl. Electrochem.* **1999**, *29*, 1.
(5) McIlroy, D. N.; Hwang, S. D.; Yang, K.; Remmes, N.; Dowben, P. A.; Ahmad, A. A.; Ianno, N. J.; Li, J. Z.; Lin, J. Y.; Jaing, H. X. *Appl. Phys. A* **1998**, 335.
(6) Yongqiang, Y. *Appl Surf. Sci.* **1998**, *140*, 19.

(7) Brust, M.; Walker, M.; Bethell, D.; Schiffrin, D. J.; Whyman, R. *J. Chem. Soc., Chem. Commun.* **1994**, 801−802.
(8) (a) Whetten, R. L.; Shafigullin, M. N.; Khoury, J. T.; Schaaff, T. G.; Vezmar, I.; Alvarez, M. M.; Wilkinson, A. *Acct. Chem. Res.* **1999**, *32*, 397. (b) Schaaff, T. G.; Shafigullin, M. N.; Khoury, J. T.; Vezmar, I.; Whetten, R. L.; Cullen, W.; First, P. N.; Gutierrez-Wing, C.; Ascensio, J.; Jose-Yacaman, M. J. *J. Phys. Chem. B* **1997**, *101*, 7885−7891. (c) Baum, T.; Bethell, D.; Brust, M.; Schiffrin, D. J.; *Langmuir* **1999**, *15*, 866. (d) Gittens, D. I.; Bethell, D.; Nichols, R. J.; Schiffrin, D. J *J. Mater. Chem.* **2000**, 79−83. (e) Luedtke, W. D.; Landman, U. *J. Phys. Chem. B* **1998**, *102*, 6566. (f) Brust, M.; Bethell, D.; Kiely, C. J.; Schiffrin, D. J. *Langmuir* **1998**, *14*, 5425−5429.
(9) (a) For a current review see Templeton, A. C.; Wuelfing, W. P.; Murray, R. W. *Acc. Chem. Res.* **2000**, *33*, 27. (b) Hostetler, M. J.; Wingate, J. E.; Zhong, C.-J.; Harris, J. E.; Vachet, R. W.; Clark, M. R.; Londono, J. D.; Green, S. J.; Stokes, J. J.; Wignall, G. D.; Glish, G. L.; Porter, M. D.; Evans, N. D.; Murray, R. W. *Langmuir* **1998**, *14*, 17. (c) Templeton, A. C.; Hostetler, M. J.; Kraft, C. T.; Murray, R. W. *J. Am. Chem. Soc.* **1998**, *120*, 1906−1911. (d) Chen, S. W.; Murray, R. W. *J. Phys. Chem. B* **1999**, *103*, 9996. (e) Templeton, A. C.; Cliffel, D. E.; Murray, R. W. *J. Am..Chem. Soc.* **1999**, *121*, 7081. (f) Green, S. J.; Stokes, J. J.; Hostetler, M. J.; Pietron, J. J.; Murray, R. W. *J. Phys. Chem. B* **1997**, *101*, 2663. (g) Chen, S.; Ingram, R. S.; Hostetler, M. J.; Pietron, J. J.; Murray, R. W.; Schaaff, T. G.; Khoury, J. T.; Alvarez, M. M.; Whetten, R. L. *Science* **1998**, *280*, 2098.

films, a study in which Au nanoparticles were attached to ordered layers of a thiolated silica colloid in a process leading to macroporous metal films. We present three approaches to metal film deposition using MPCs. One involves a step-by-step chemical attachment of multilayers of MPCs to a glass substrate, tracked by UV–vis absorbance and based on recently described[11] Cu^{2+}–carboxylate coordinative linkage chemistry. These MPCs have mixed monolayers of alkanethiolates and ω-carboxyl-alkanethiolates. Following MPC film formation, thermolysis of the MPC multilayers at temperatures <300 °C to volatile disulfides[9b] yields 5–100-nm-thick, strongly adherent, metal films. A second procedure simply deposits alkanethiolate MPCs by casting or painting a solution of them onto the substrate, again followed by thermolysis to produce somewhat less adherent 500–1000-nm films. The third procedure involves an electrochemically generated destabilizer (iodide) that decomposes the MPC monolayer (either *N*-(2-mercaptopropionyl)glycine (tiopronin) or alkanethiolate) to deposit a metal film onto the electrode.

A thermal desorption mass spectrometric study[9b] established that the MPC monolayers decompose to volatile disulfides. The current and potential diversity of metals[12] and their alloys[13] in MPC cores, the simplicity of MPC synthesis, and the ease of their storage as solids led us to consider their broader potential as metal film precursors. Coatings prepared from contact of solutions with the substrate surface offer attributes of forming deposits on samples with complex three-dimensional surfaces and of tailoring substrate surface chemistry for good adhesion properties. We have applied a battery of analytical methods to characterize the metal films produced, including UV–vis spectroscopy, scanning electron microscopy (SEM), energy-dispersive X-ray analysis (EDX), X-ray photoelectron spectroscopy (XPS), stylus profilometry, and atomic force microscopy (AFM).

Experimental Section

MPC Synthesis. MPCs were prepared as previously described.[9b,12–14] There are variations to this procedure including those for synthesis of MPCs with cores of metal alloys[13] and of MPCs with tiopronin monolayers.[15] MPCs with mixed hexanethiolate/ω-mercaptoundecanoic acid monolayers were prepared by place-exchange reactions[16] between hexanethiolate MPCs and ω-mercaptoundecanoic acid.

Films Based on Coordinatively Assembled MPC Multilayers: MPC Substrate Preparation ((3-Mercaptopropyl)trimethylsiloxane (MTMS) Glass Derivatization), MPC Multilayer Formation, and Thermolysis. We fol-

lowed the general procedure by Majda and co-workers[17] to derivatize precut (≈3 × 1 cm) Fisher *Finest* brand microscope slides with this adhesion-promoting, thiolated silanizing reagent. The detailed procedure is given in the Supporting Information.

For assembly of a Au MPC multilayer, the general procedure is that the freshly derivatized glass slide placed in 0.1 M Cu(ClO₄)₂/ethanol solution is removed after 1 h, rinsed copiously with ethanol, and placed into a dilute (≈50 μM, 2 mg/mL) ethanol solution of a mixed hexanethiolate/ω-mercaptoundecanoic acid monolayer MPC, such as $Au_{140}(SC6)_{30}(SC10COOH)_{23}$, for 1 h. Again, the slide is rinsed copiously with ethanol, blown dry with N_2 gas, and the MPC film absorbance measured at 400 nm. This constitutes one cycle of multilayer MPC film formation as described in Figure 1. This procedure, which forms the equivalent of 20–50 monolayers of attached MPCs, is repeated, starting again with the 0.1 M Cu(ClO₄)₂/ethanol solution, until the desired MPC film thickness is obtained as judged by the 400-nm absorbance.

The MPC multilayer films were placed in a Thermolyne 1500 electric furnace at 250 °C or greater for 5 min, leaving the furnace cover ajar to allow gaseous MPC decomposition products to escape. Within the first minute of thermolysis, the film changes from its black coloration to a shiny metallic appearance. Films were thermolyzed at various temperatures from 250 to 350 °C.

Films Based on Cast MPC Multilayers: Substrate Preparation, Drop-Casting, and Thermolysis. Glass slides were cleaned by sonication in a soap solution and exposure to pirhanna solution (2:1 H_2SO_4:H_2O_2 (30% solution), use caution). After the surface was blown dry with N_2 gas, films of alkanethiolate MPCs were immediately drop-cast from concentrated (25 mg/mL, ≈1.5 mM) MPC/toluene solutions, allowing each drop to dry (≈1 min) before adding another—up to five drops. After air-drying for ≈10 min, the slides were placed in the electric furnace at 300 °C for 0.5 h (cover ajar). The slides were allowed to cool to room temperature and stored in a closed container. The films were rinsed with 10 mL of 2-propanol before SEM, EDX, and XPS experiments.

Electrochemical Deposition of Metal Films from MPCs. A 0.6-mm-radius Pt electrode was polished with 0.25-μm diamond paste and cleaned by cycling in dilute H_2SO_4 for 10 min. This electrode was then placed into an aqueous 0.05 M KIO_3/10 μM Tiopronin-MPC solution with a Pt coil counter and a SSCE reference. Electrochemistry was performed on an EG&G PAR 277A potentiostat.

Characterization Experiments. Scanning electron microscopy (SEM) was carried out on a Cambridge S200 instrument at ≈10^{-7} Torr, 25-keV beam energy, and ≈0.8-nA beam current. Images were acquired with the sample stage tilted 45° from the horizontal sample position. Energy-dispersive X-ray analysis (EDX) was performed with a Kevex 7000 energy-dispersive spectrometer with a 4π interface. X-ray photoelectron spectroscopy (XPS) was performed with a Physical Electronics (PHI) Model 5400 equipped with a hemispherical analyzer and a Mg Kα source operating at an energy of 15 keV and 400 W. The survey spectra were taken with a pass energy of 89.54 eV, and for angle-resolved XPS (AR-XPS), with takeoff angles of 15°, 45°, and 75°. The analysis area of the metal films was 1.1 mm² with a typical operating pressure of 10^{-8} Pa. Binding energies are referred to the adventitious carbon C1s peak at 284.6 eV. Alloy film atomic ratios were calculated by using XPS and empirically derived sensitivity factors.[18] Film thickness determinations by stylus profilometry were performed using a Tencor Alpha-Step 100. Electrochemical data were taken with an EG&G PAR 277A potentiostat, UV–vis spectra with a ATI Unicam spectrometer (using a MTMS-derivatized glass slide as the reference), and contact mode AFM images with a Nanoscope II (Digital Instruments, Santa Barbara, CA) with silicon nitride tips.

(10) Jiang, P.; Cizeron, J.; Bertone, J. F.; Colvin, V. L. *J. Am. Chem. Soc.* **1999**, *121*, 7957.

(11) Zamborini, F. P.; Hicks J. F.; Murray, R. W. *J. Am. Chem. Soc.* **2000**, *122*, 4514.

(12) Hostetler, M. J.; Murray, R. W., unpublished results, University of North Carolina.

(13) Hostetler, M. J.; Zhong, C.-J.; Yen, B. K. H.; Anderegg, J.; Gross, S. M.; Evans, N. D.; Porter, M.; Murray, R. W. *J. Am. Chem. Soc.* **1998**, *120*, 9396.

(14) Chen, S.-W.; Templeton, A. C.; Murray, R. W. *Langmuir* **2000**, *16*, 3543.

(15) (a) Templeton, A. C.; Chen, S.; Gross, S. M.; Murray, R. W. *Langmuir* **1999**, *15*, 66. (b) Templeton, A. C.; Cliffel, D. E.; Murray, R. W. *J. Am. Chem. Soc.* **1999**, *121*, 7081.

(16) Hostetler, M. J.; Templeton, A. C.; Murray, R. W *Langmuir* **1999,** *15*, 3782.

(17) Goss, C. A.; Charych, D. H.; Majda, M. *Anal. Chem.* **1991**, *63*, 85.

(18) Chastain, J. *Handbook of X-ray Photoelectron Spectroscopy*; Perkin-Elmer: New York, 1992.
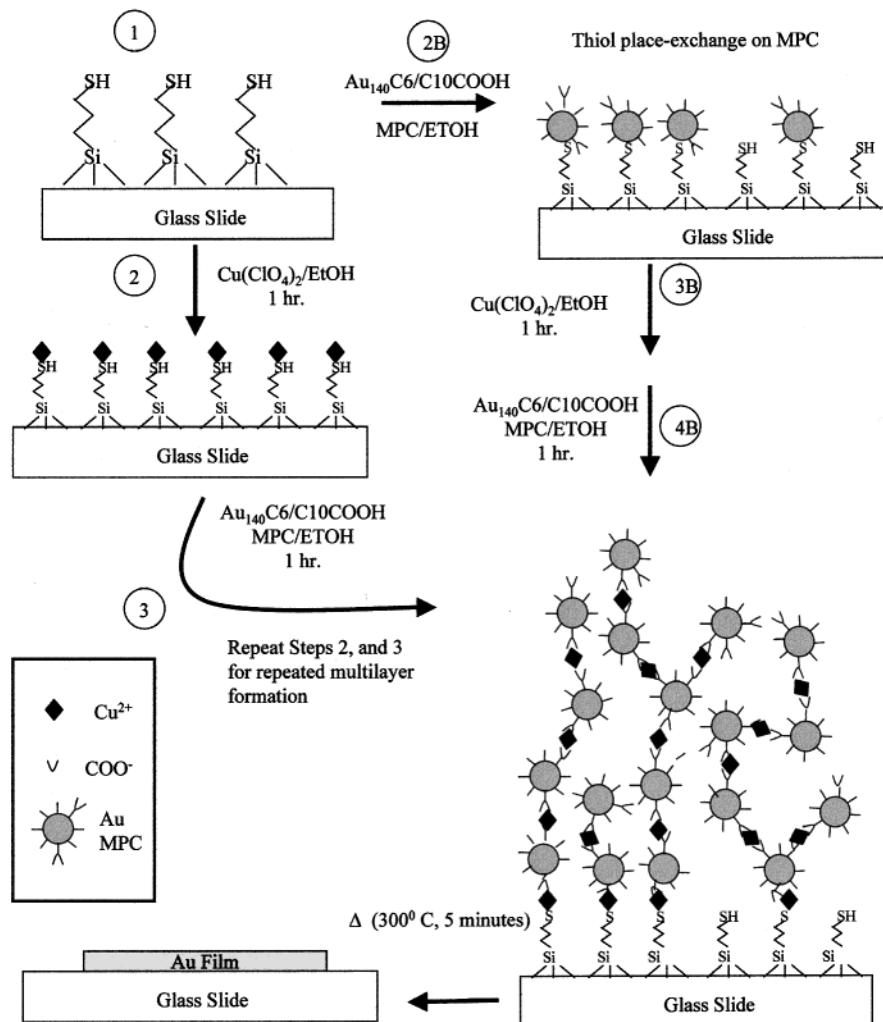
Figure 1. Schematic describing the assembly method and the following thermolysis of an assembled film.

Results and Discussion

Most MPC research to date has involved either the chemistry of the monolayer or the electronic properties of the nanoparticle itself.[8,9] The experiments described here utilize the MPC as nanometer-sized building blocks for metal films and are only starting points; no attempt was made to optimize films for any particular use.

Step-by-Step MPC Multilayer Film Assembly and Characterization. *Multilayer Film Assembly.* Multilayer films of nanoparticles that are coated with mixed hexanethiolate/ω-mercaptoundecanoic acid monolayers (abbreviated C6/C10COOH) can be prepared[16] by the two-reaction pathways illustrated in Figure 1. Both pathways begin with a thiolated surface such as the glass surface in Figure 1 (step 1) that had been reacted with (3-mercaptopropyl)trimethylsiloxane (MTMS), followed by steps 2 and 3 or 2B−4B. In step 2, the thiolated surface is metalated with Cu^{2+} ions (based on a report by Bard and co-workers[19]). Exposing this surface to a solution of the mixed monolayer MPC leads (step 3) to accumulation of a multilayer film of MPCs ($\approx$30 layers depending on the length of MPC exposure), which is readily monitored by UV−vis spectroscopy.[20] Steps 2 and 3 can be serially repeated many times to build the MPC film to a desired thickness. The second pathway,

steps 2B−4B in Figure 1, is equally effective, but slower. The thiolated glass surface is incubated in a MPC solution so as to attach a partial monolayer of MPCs by a place exchange reaction (displacing a hexanethiolate ligand),[16] followed by steps 3B and 4B (which are the same as steps 2 and 3).

Formation of a multilayer of MPCs in a single exposure to the MPC solution (step 3) means that the initial ca. monolayer of Cu^{2+} ions on the thiolated surface must become redistributed.[21] Adding these layers of MPCs to the growing film requires the presence of the metal ion, which binds MPCs into the film with coordinative carboxylate/Cu^{2+}/carboxylate bridges. No film growth occurs without a metal ion present. The continued multilayer growth that occurs upon repetition of steps 2 and 3 is presumably driven by Cu^{2+} incorporated into the film in step 2 by metalation of carboxylate

(19) Brust, M.; Blass, P. M.; Bard, A. J. *Langmuir* **1997**, *13*, 5602.

(20) (a) The molar absorbance coefficient, $\epsilon = 4 \times 10^5$ M^{-1} cm^{-1}, is used in the equation, $A = 10^3 \epsilon \Gamma$, where Γ is MPC coverage in mol/cm^2. Γ is converted into numbers of monolayers based on $\Gamma_{MONOLAYER} \approx 2 \times 10^{-11}$ mol/cm^2, which is based on a hexagonal close-packed model[15b] in which the Au_{140} nanoparticle core diameter is 1.6 nm and a fully extended mercaptoundecanioc acid chain is 1.77 nm (via modeling software). The nanoparticle diameter and thickness per MPC monolayer is thus modeled as 5.14 nm. Account is taken of the fact that the MPC film grows on both sides of the glass slide. The molar absorbance was determined from $Au_{140}C6_{53}$ MPC solutions.

(21) It is unclear at this point whether the Cu^{2+} is redistributed by some solvent (EtOH) mechanism or if the ion can move in the film.
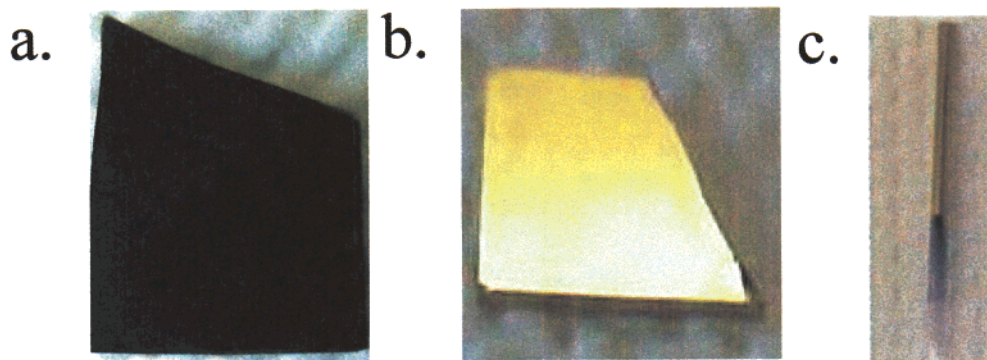
Figure 2. (a) Photograph of a Cu^{2+} assembled MPC film. The black appearance is due to the strong absorbance of the MPCs in the visible region of the spectrum. (b) Photograph of a thermolyzed assembled film. (c) Photograph of a thermolyzed assembled film on a pipet tip. The images are roughly 2-cm long.

groupings not already involved in bridging. The process of Cu^{2+} migration through MPC multilayers seems to be moderately slow, as judged by the fact that multilayer film growth is promoted by longer soaking times (up to ≈ 1 h) in steps 2 and 3. Further study is underway on the multilayer film growth kinetics.

MPCs used in experiments reported had the average composition $Au_{140}(SC6)_{30}(SC10COOH)_{23}$ and are heavily loaded with carboxylate groups. Each MPC can accordingly be expected to contain multiple Cu^{2+}-based coordinative bridges to other MPCs. Multilayer films can nonetheless be grown from MPCs having much lower loadings of the ($-SC10COOH$) ligand; we are still exploring the properties of such films. The growth process also has interesting peculiarities; film growth sometimes abruptly stops between $A = 2$ and $A = 4$, which raises the possibility that sometimes the top surface of the multilayer has an insufficient amount of exposed carboxylate groups. MPC multilayers can also be grown using other metal ions, such as Zn^{2+}, Pd^{2+}, Fe^{2+}, and Ag^+. Specific details of film growth vary with the metal; for example, Zn^{2+} is an effective bridging metal only if the MPC carboxylates are first deprotonated, whereas this is unnecessary and without effect for Cu^{2+}.

As multiple MPC multilayers are grown through repetitions of steps 2 and 3 (or 3B and 4B), the glass slide is perceptibly darkened and in some cases, as in Figure 2a and 3, after eight repetitions is completely opaque, appearing as a shiny black film. Figure 2a shows a photo of such a film assembled using Cu^{2+}. Because the entire glass surface had been thiolated, the MPC multilayer formed over the entire glass slide surface, including the sharp corners, and curved edges. The films are adherent and mechanically quite stable, passing "tape" testing like that used by Crooks et al.[22] to characterize Au film adhesion. Scraping the film with a sharp metal object succeeds in removing only small amounts of the material. At the same time, the MPC film formation is chemically reversible; MPC multilayers are completely dissolved by acid (acetic) and by strong Cu^{2+} ligands such as thiols, both steps serving to destabilize the Cu^{2+}-carboxylate coordination.

Electronic Spectra. Figure 3 spectra show consecutive repetitions of the $Au_{140}(SC6)_{30}(SC10COOH)_{23}/Cu^{2+}$ film
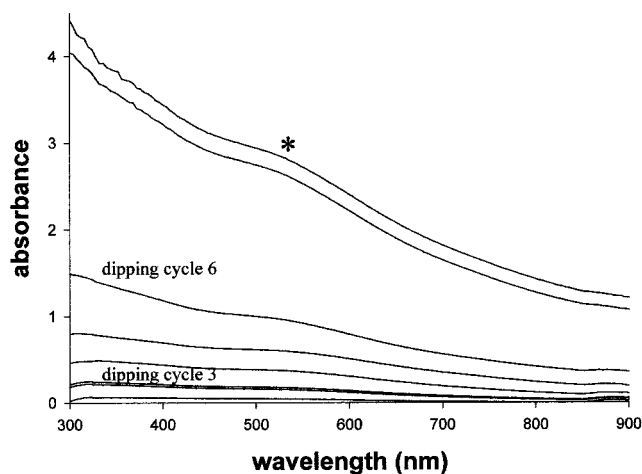

Figure 3. UV–vis spectra of Cu^{2+} assembled MPC film growth. Each spectrum was taken after a dipping cycle (several hours in MPC and Cu^{2+}) as described in Figure 1. (*) marks the surface plasmon (SP) band for the film.

growth process using steps 2 and 3 from Figure 1. Film thickness is estimated spectrophotometrically[20] at 400 nm using $\epsilon = 4 \times 10^5$ M^{-1} cm^{-1} for $Au_{140}(SC6)_{53}$ MPCs; the maximum absorbance attained in Figure 3 (400 nm) corresponds to a total film height of 2.1 μm or ≈ 400 monolayers of MPCs. This value is the summation of absorbance from both sides; thus, we estimate equal growth on each side or ≈ 1.1 μm in thickness. Stylus profilometry of this MPC film gave a similar film thickness of 1.0 μm (on each side of the glass slide). The $\approx 10\%$ correlation between the spectroscopic and profilometry data means that the model assumption that linker chains are on average fully extended[20] is reasonable. More densely packed films should result with shorter linker chains. Thus far, we have grown films over an absorbance (400 nm) range from 5 to <0.1.

Metal nanoparticles often exhibit surface plasmon (SP) optical absorptions due to surface electronic excitations. These lie at 518–520 nm for Au MPCs, are weak, and diminish with nanoparticle size. For the Au_{140} MPCs (1.6-nm average core diameter), the SP band is extremely faint[23] to nonexistent.[9a,b] For slightly larger nanoparticles having tiopronin monolayers that possess carboxylate functionality, the weak SP band undergoes

(22) Baker, L. A.; Zamborini, F. P.; Sun, L.; Crooks, R. M. *Anal. Chem.* **1999**, *71*, 4403.

(23) Hicks, J. F.; Murray, R. W., unpublished results, University of North Carolina.
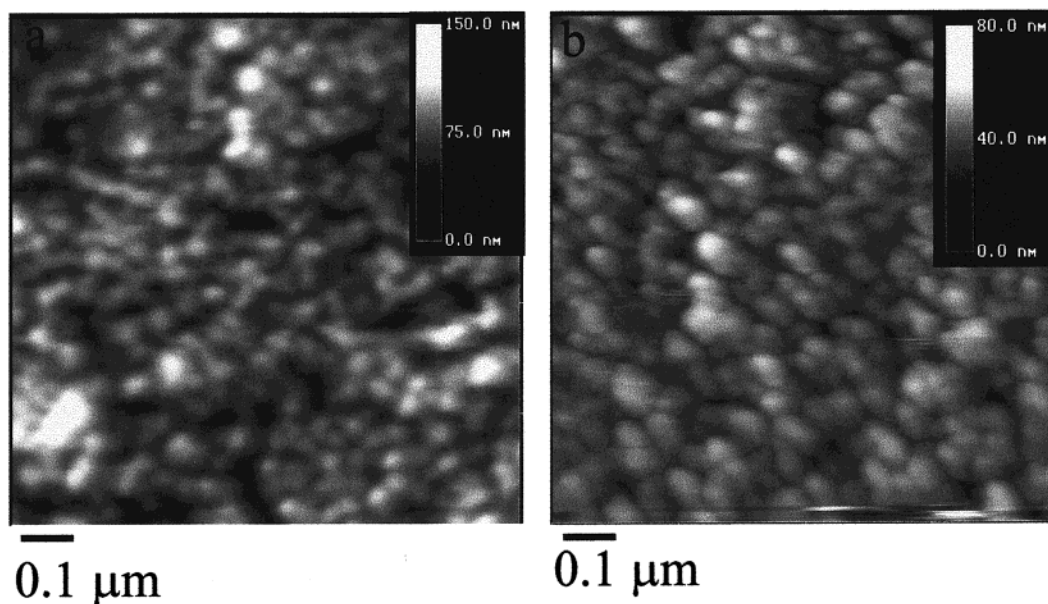
Figure 4. AFM images of (a) assembled $Au_{140}(SC6)_{33}(SC10COOH)_{23}$ /Cu^{2+} MPC film and (b) thermolyzed assembled MPC film.

a red shift of a few tens of nanometers when clustering of the MPCs is induced by adding Cu^{2+} to very dilute solutions.[24a] Spectra of precipitated MPCs or of MPCs dispersed in nonsolvents exhibit further red-shifted bands,[24a] called aggregation or collective SP bands. Because of the stated chemical reversibility of the carboxylate binding, aggregation denoted by the red shift does not imply that the nanoparticle cores themselves have aggregated.

Spectra of MPC multilayers exhibit an enhancement of the SP band and small red shifts that range from 524 to 540 nm. In Figure 3, the SP band lies at 530 nm (*). In similar work by Natan[24b] surface aggregation of larger colloids showed red-shifted SP bands. The spectral trend seen simply shows that the cores have been brought into closer proximity than those in solution spectra; here, they act somewhat like larger core MPCs. However, the relatively small effect indicates that the monolayer and Cu^{2+}/carboxylate bridging structures maintain spacing between the Au cores. This is consistent with the observations of film thickness and of the dissolution properties of the films (vide supra).

AFM Imaging of MPC Multilayers. Figure 4a shows an AFM image of the Cu^{2+}-assembled MPC multilayer employed in Figure 3. The RMS surface roughness, $\approx$10 nm, is larger than that of an evaporated metal film ($\approx$2−4 nm),[22,25] and the MPCs appear to have become beaded together into roughly spherical units $\approx$10 MPCs in diameter (equivalent to around 400 MPCs/"bead"). The basis of the beaded morphology in Figure 4a, and whether it is representative of much thinner MPC multilayers, is unknown at present. The image also shows occasional dendritric-like "towers" scattered over the surface (Figure 4a) that are several beads high. The dark regions in the figure appear to be void spaces.

Thermolysis of Step-by-Step Assembled MPC Multilayers and Characterization of Metal Films.

Thermolysis. Thermolysis of the multilayer MPC films produces reflective metal films that are visually comparable to evaporated films.[26] The color is slightly more yellow than evaporated Au, which may be ascribed to their Cu content. We use below a notation of Au/Cu for a film formed from thermolysis of a film containing $Au_{140}(SC6)_{30}(SC10COOH)_{23}$ and Cu^{2+}. The Au/Cu film is nominally an alloy but the spatial distribution of the two metals is unknown.

A potentially important aspect of the MPC film assembly is an ability to *coat curved and enveloped surfaces* and the consequent ability to metallize such surfaces. Figure 2b,c show two simple examples where an irregularly fractured glass slide has been coated with a Au/Cu film on the flat, edges, and corners and the tip of a micropipet has been coated inside and outside. The ability to coat surfaces that are accessible to solutions but otherwise occluded may offer advantages over more conventional modes of metal deposition, such as generating nanometer-sized ring electrodes.

The metal films are, furthermore, strongly adherent as shown in "tape tests", which remove little to none of the Au/Cu metal film. The good surface adhesion cannot be ascribed to chemical anchoring by the MTMS ligand as it should be decomposed during thermolysis. Also, a film exposed to a H_2/O_2 flame for several seconds continued to exhibit strong adhesion (see Supporting Information).

Characterization of Thermolyzed Films. The alkanethiolate volume fraction of an MPC is large, about 80%, so it is unsurprising that the films become much thinner following thermolysis. The MPC film spectrophotometrically estimated as 1.1-μm-thick per side in Figure 3 gave, following thermolysis, a 0.11-μm-thick metal film (by profilometry). AFM images are shown in Figure 4b. The morphology is somewhat smoother than the precursor MPC multilayers; the RMS roughness is now 6−7 nm and the incidence of dendritic-like towers is sharply lowered. The beady structure of the MPC multilayer

(24) (a) Templeton, A. C.; Zamborini, F. P.; Wuelfing, W. P.; Murray, R. W. *Langmuir* **2000**, *16*, 6682−6688. (b) Brown, K. R.; Lyon, L. A.; Fox, A. P.; Reiss, B. D.; Natan, M. J. *Chem. Mater.* **2000**, *12*, 314.
(25) Hegner, M.; Wagner, P.; Semenza, G. *Surf. Sci.* **1993**, *291*, 39.

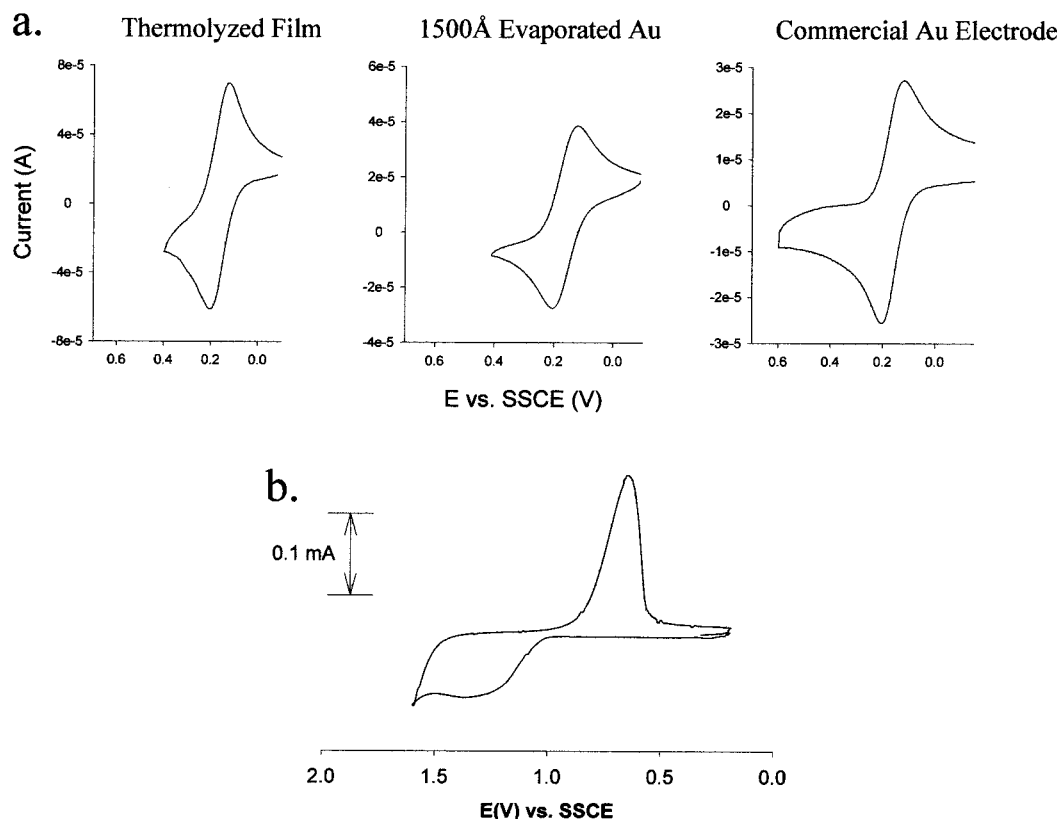(26) Comparable to those made from an Edwards Auto 306 metal evaporator.

a.

| Thermolyzed Film | 1500Å Evaporated Au | Commercial Au Electrode |

E vs. SSCE (V)

b.

0.1 mA

E(V) vs. SSCE

Figure 5. (a) Cyclic voltammetry (20 mV/s) of 0.1 mM $K_2Fe(CN)_6$ in aqueous 0.1 M $NaClO_4$ at a 20-nm-thick per side electrode prepared by thermolyzing a $Au_{140}(SC6)_{33}(SC10COOH)_{23}/Cu^{2+}$ MPC film ($\approx$112 mm²) and cleaned by potential cycling in 0.1 M H_2SO_4 for 10 min, a 0.15-μm Au film evaporated (10-nm Cr adhesion layer) on glass (150 mm²), and a 2-mm-diameter BAS macroelectrode polished with a 0.25-μm diamond slurry and cleaned by potential cycling in 0.1 M H_2SO_4 for 10 min. (b) Cyclic voltammetry (200 mV/s) of the thermolyzed film electrode used in (a) in 0.1 M $HClO_4$.

persists, but comparison between parts a and b of Figure 4 suggests that some bead fusion has occurred. It is worth reminding the reader that the thermolysis temperature is far below the softening point of the Au/Cu metals. Whether the void structures evident in Figure 4a diminish after thermolysis is unclear; the dark lines in Figure 4b may be persisting voids or new ones that opened by strain associated with the change in film volume.

Cyclic voltammetry with thermolyzed Au/Cu metal film electrodes is illustrated in Figure 5. Figure 5a shows $Fe(CN)_6^{4-/3-}$ voltammetry at a thermolyzed Au/Cu film, a-150 nm evaporated Au film, and a conventional "bulk" Au electrode. The thermolyzed electrode is $\approx$40-nm-thick judging by its prethermolysis 400-nm thickness.[20] The thermolyzed electrode voltammogram is well-formed, stable over a period of several hours, and slightly more reversible (ΔE_{PEAK} = 70 mV) than the other two (ΔE_{PEAK} = 82 and 74 mV for the evaporated and commercial electrode, respectively). That the thermolyzed electrode shows no voltammetric evidence of copper is unsurprising given the H_2SO_4 electrode-cleaning procedure employed. Gold oxide film formation on the same thermolyzed film is illustrated in Figure 5b by a broad oxidation wave and the subsequent, reduction stripping wave. The voltammogram is quite similar to that of polycrystalline Au.[27] The $\approx$40-nm film
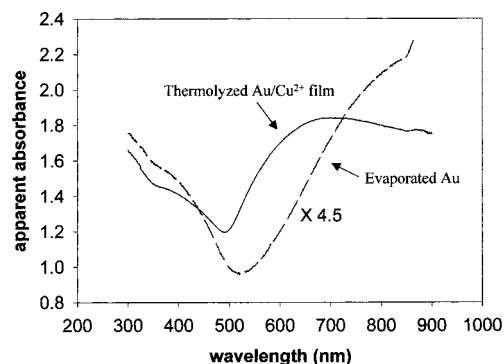
(27) (a) Trevor, D. J.; Chidsey, C. E. D.; Loiacono, D. N. *Phys. Rev. Lett.* **1989**, *62*, 929. (b) Angerstein-Kozlowska, H.; Conway, B. E.; Hamlelin, A.; Stoicoviciu, L. *J. Electroanal. Chem.* **1987**, *228*, 429.

Figure 6. UV−vis spectra of a thermolyzed MPC film (0.3 μm per side by profilometry) (−) and a 100-Å evaporated Au film on glass (− −). The evaporated Au signal is multiplied by a factor of 4.5.

visually thinned on some areas upon prolonged potential cycling (>2000 cycles at 200 mV/s over a 100-min period), showing that even a very thin thermolyzed Au/Cu film is electrochemically robust and well-behaved.

Optical transmission spectra of thermolyzed films are quite different from those of the MPC multilayers (Figure 3), as shown in Figure 6 (− −) for a thermolyzed Au/Cu film (0.3-μm-thick on each side by profilometry). The overall absorbance is lower and there is the pronounced minimum in absorbance common to thin Au films.[28] Throughout these experiments, thermolyzed film absorbance minima lie at 493 nm (±2); for comparison the absorbance minimum of a 10-nm-evaporated Au film, Figure 6(− −), has a 34-nm-higher wavelength.

The absorbance of thin films is dominated by the changing refractive index over the UV–vis spectrum; the incorporation of Cu into the film may simply shift the well-known[28a,c] drop-off in refractive index in thin Au films to higher wavelengths. Preliminary experiments on thermolyzed films prepared using other ions such as Fe^{2+}, Pd^{2+}, and Ag^+ reveal other shifts of absorbance minimum and differing spectral envelopes. The ability to control the optical transmission properties of the thin metal films is interesting and may offer some usefulness as, for example, in surface plasmon resonance measurements.[29]

Scanning electron microscopy (SEM) images of thermolyzed MPC films are shown and discussed in the Supporting Information—in general, they match the AFM images. Energy-dispersive X-ray analysis (EDX) interestingly shows only slight Cu levels above the baseline, suggesting that the carboxylates are less than fully metalated.

Thermolysis of Cast MPC Films. Metal films can also be produced simply by thermolysis of MPC films that had been drop-cast from solutions; this approach was investigated prior to the step-by-step procedure discussed above. The MPCs used included Au, Ag, Pd, and MPCs with alloy cores.[13] Three-dimensional substrates can also be coated, by dipping. In general, metal films prepared from cast or dipped MPC films were much thicker, but less adherent (fail a "tape test"), than those prepared with the step-by-step procedure. Stylus profilometry showed a thin periphery (≈ 1 μm) and thicknesses of up to 15 μm in the film interiors. Films made using MPCs with a single core metal were substantially smoother than those made from alloy-core MPCs, some of which displayed a porous-looking morphology when viewed by SEM. The monometal films are described with SEM and EDX in the Supporting Information. Because there are no prior reports of thermal decomposition of alloy MPCs to alloy films, we wished to particularly characterize their behavior.

Films from MPCs with Alloy Cores. Metal alloy films have been produced by a variety of methods in the past.[30] Thermolysis of these MPCs amounts to producing alloys from alloy precursors, which differs from previous approaches. We again employ alloy MPCs of AuAg, AuCu, AgPd, and AuAgCuPd that had been previously characterized by XPS and elemental analysis.[12,13] The cast MPC-film approach was employed, although we expect in the future to adapt the step-by-step method to gain improved adhesion.

XPS analysis of the thermolyzed alloy MPCs imitates the results from the precursor alloy MPCs in that XPS shows that surface compositions differ from the bulk, indicative of segregation. SEM reveals substantial surface roughness, an interesting result considering the smoothness of similarly prepared single-metal films.

Table 1. XPS Surface Analysis of Thermolyzed Drop-Cast MPC Films

MPC precursor/ (metal ratio)[a]/ core diameter[c]	takeoff angle (deg)	Au	Ag	Cu	Pd
AuCu	15	1		5.4	
(1/1)[a]	45	1		4.2	
1.5 nm[c]	75	1		4.1	
AuAg	15	1	1.0		
(1:0.9)[b]	45	1	1.0		
2.2 nm[c]	75	1	0.9		
AgPd	15		1		0.5
(1:1)[a]	45		1		0.6
1.7 nm[c]	75		1		0.5
AuAgCuPd	15	1	0.6	0.9	1
(1:1:0.1:3)[b]	45	1	0.6	0.9	0.7
1.7 nm[c]	75	1	0.5	0.6	0.8

[a] Elemental analysis results (see ref 13). [b] Calculated from MPC XPS results (ref 13). [c] From transmission electron microscopy (usually ±25%).

Like the monometal films, EDX spectra (Figure S-4) exhibit peaks for the metal alloy constituents. Accounting for instrument sensitivity factors and reference standards,[31] the relative EDX peak intensities for both the AuCu and AuAg alloy films give a 1:1 metal ratio, close to the previous elemental analyses (1:1 and 1:0.9, respectively, see Table 1) of these alloy MPCs. For AgPd films, the thermolyzed film EDX gave a 1.5:1 ratio not in good agreement with the 1:1 precursor alloy MPC analysis. The quaternary alloy EDX result for Au:Ag: Cu:Pd was 1:1:0.02:0.6, which is lean in Cu and Pd given the previous elemental analysis 1:1:0.1:3 of the alloy MPC.

Angle-resolved XPS was applied to the thermolyzed alloy MPC films using 75°, 45°, and 15° takeoff angles, which probe, roughly, the first 40, 30, and 10 Å of the films, respectively.[32] Atom ratio results are given in Table 1 and BE in Table S-2. The precursor AuCu alloy MPC, while having an overall MPC core 1:1 Au:Cu molar composition, had been previously determined[13a] by XPS to have a 1:3.7 Au:Cu concentration—that is, the precursor MPC surface was enriched in Cu. The same result is obtained here (Table 1) in XPS of the surface of the thermolyzed alloy MPC film, where an even higher proportion of Cu was found at the surface at the shallowest (15°) takeoff angle. As found before[13] for the intact alloy MPCs, the BE of the two metals are consistent (Table S-2) with zerovalent Au and copper oxide. In thermolyzed AuAg alloy MPCs, both metals again have zerovalent-like BE, but the 1:2.2 Au/Ag surface enrichment[13] (versus elemental analysis) in the precursor alloy MPCs is not observed in the alloy film, whose XPS—like the EDX—gives a 1:1 surface atom ratio. It would seem that, whatever aspect of the alloy MPC synthesis produces a Ag surface enhancement on individual Au/Ag MPCs is on average lost when a large

(28) (a) Khawaja, E. E.; Durrani, S. M. A.; Al-Shurki, A. M. *Thin Solid Films* **2000**, *358*, 166. (b) Aspenes, D. E.; Kinsbron, E.; Bacon, D. D. *Phys. Rev. B* **1980**, *21*, 3290. (c) *American Institute of Physics Handbook*, 3rd ed.; McGraw-Hill: New York, 1972; pp 6–138.

(29) (a) Nelson, B. P.; Frutos, A. G.; Brockman, J. M.; Corn, R. M. *Anal. Chem.* **1999**, *71*, 3928. (b) Frutos, A. G.; Weibel, S. C.; Corn, R. M. *Anal. Chem.* **1999**, *71*, 3935.

(30) (a) Zhang, Y. P.; Puddephatt, R. J. *Chem. Mater.* **1999**, *11*, 148. (b) Adurodija, F. O.; Song, J.; Kim, S. D.; Kwon, S. H.; Kim, S. K.; Zell, D.; Yoon, K. H.; Ahn, B. T. *Thin Solid Films* **1999**, *338*, 13. (c) Saidman, S. B.; Munoz, A. G.; Bessone, J. B. *J. Appl. Electrochem.* **1999**, *29*, 245.

(31) Desktop Spectrum Analyzer DTSA v. 2.5 software. The ionization efficiency differences between Cu and the other elements present in the AuCu and AuAgCuPd films require a known reference percentage within the film to provide the semiquantification. When the estimated (from MPC precursor) percentage of copper in the films was employed in the calculation, the other percentages of the metal within the film agreed with the XPS results and original nanoparticle composition.

(32) (a) Tanuma, S.; Powell, C. J.; Penn, D. R. *Surf. Interface Anal.* **1991**, *17*, 911. (b) Powell, C. J.; Jablonski, A.; Tilinin, I. S.; Tanuma, S.; Penn, D. R. *J. Electron Spectrosc. Relat. Phenom.* **1999**, *98*, 1.
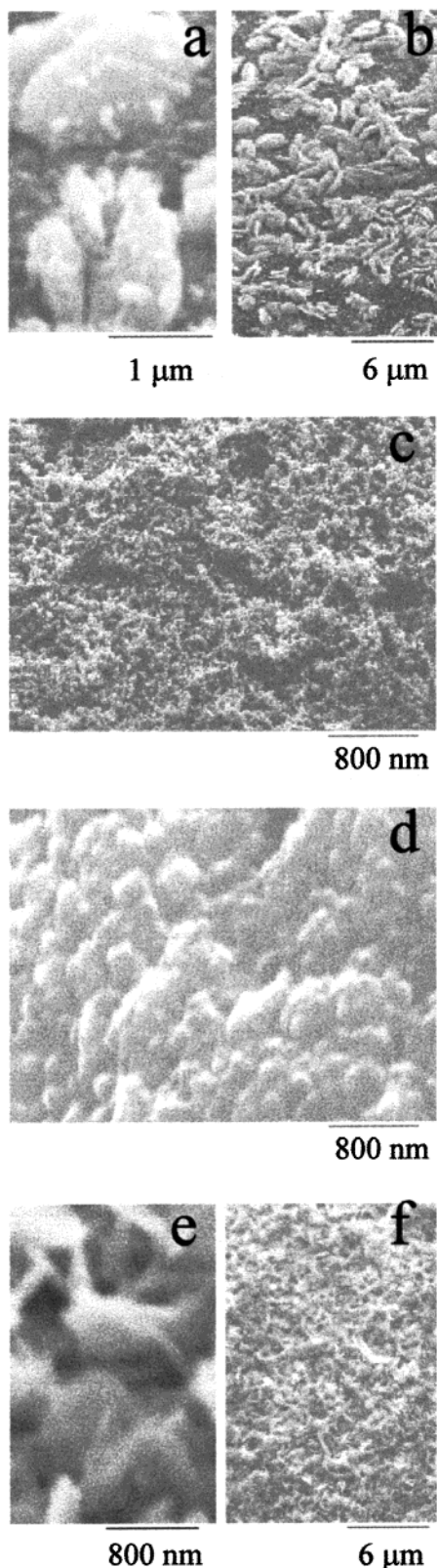
Figure 7. SEM photomicrographs for the alloy metal film preparations: (a) and (b) AgPd; (c) AuAg; (d) AuCu; (e) and (f) AuAgCuPd.

array of MPCs is thermally decomposed, while the Cu constituent of the alloy retains its driving force for surface accumulation by way of its oxiding characteristic.

AgPd film (1.5:1 by EDX) analysis revealed a rather angle-independent metal ratio of $\approx$1:0.5 at all three takeoff angles showing a preference of Ag at the surface compared to the bulk composition. The binding energies of Ag and Pd metals were consistent with those in the single-metal films (Ag and PdO). The elemental analysis-determined precursor MPC composition was 1:1 Ag:Pd.[33]

The precursor AuAgCuPd MPCs had a metal ratio of 1:1:0.1:3 as determined by elemental analysis; the Cu component is presumed[13] to have been depleted in the alloy by galvanic action during the synthesis. XPS analysis of the thermolyzed alloy film formed from this quaternary alloy MPC shows that the small amount of Cu has been drawn to the alloy film surface; again, oxides are formed as indicated from the Cu and Pd BE data. The other metals are in elemental form. The level of organic contamination in the alloy films was comparable to those of the monometal films (discussed in the Supporting Information).

SEM images of thermolyzed alloy MPCs reveal substantial morphological differences from the Au/M and monometal films. The Figure 7 images are typical of two different alloy film batches studied. Figure 7a,b of a AgPd film reveals the presence of a well-defined surface structure, and on the coarser scale, well-developed surface lumps are evident over the entire film surface. The AuAg film (Figure 7c) has an extremely roughened, or pitted, surface and at larger scales looks very uneven. The AuCu film in Figure 7d is the smoothest of the alloys, agreeing with the relative smoothness of the Au/Cu results, while the AuAgCuPd alloy film (Figure 7e and 7f) is almost porous in appearance.

The reason(s) for the roughening of the alloy films, relative to that of single-metal films, can only be speculated about at this point. The literature, however, does indicate that alloy films can be roughened in comparison to films of single-metal constituents.[34] One plausible origin could be the surface energy factors that drive metal surface segregation; the surface energy depression attendant to metal segregation would also tend toward maximizing the quantity of surface formed during MPC metal core aggregation.

Electrochemical Deposition. A third method of metal deposition from electrochemical decomposition of the monolayer is described in the Supporting Information.

Conclusions

This report demonstrates simple methods for preparing single-metal and alloy films under standard atmospheric conditions for planar, curved, and electrode surfaces. The ability to utilize MPCs as stable metal sources make them attractive for metal film design on substrates and opens the possibility to (a) prepare solid metal films from MPC precursors for decorative purpose, (b) prepare solid electrodes with atypical geometry, (c) prepare thin films with unique optical properties, and (d) set the groundwork for the more careful exploration of MPCs as precursors to metal films on various substrates such as polymers or other metals. The major

(33) No XPS data were available on this MPC for surface segregation information.

(34) (a) Nakajima, T.; Koh, M.; Sign, R. N.; Shimada, M. *Electrochim. Acta* **1999**, *44*, 2879. (b) Craciun, R. *Solid State Ionics* **1998**, *110*, 83. (c) Latha, G.; Rejendran, N.; Rajeswari, S. *J. Mater. Eng.* **1997**, *6*, 743. (d) Komori, M.; Akiyama, E.; Habazaki, H.; Kawashima, A.; Asami, K.; Hashimoto, K. *Appl. Catal. B* **1996**, *9*, 93.

constraint at this point is the presence of surface contamination, which should be reduced by further experimental design such as by active removal of MPC decomposition byproducts.